Supplementary information – Figures and Tables

Impact of coagulation-ultrafiltration on long-term pipe biofilm dynamics in a full-scale chloraminated drinking water distribution system

Kristjan Pullerits[a,b], Sandy Chan[a,b,1], Jon Ahlinder[c], Alexander Keucken[d,e], Peter Rådström[a], Catherine J. Paul[*,a,e]

[a]Applied Microbiology, Department of Chemistry, Lund University, P.O. Box 124, SE-221 00 Lund, Sweden

[b]Sweden Water Research AB, Ideon Science Park, Scheelevägen 15, SE-223 70 Lund, Sweden

[c]FOI, Swedish Defence Research Agency, Cementvägen 20, SE-906 21 Umeå, Sweden

[d]Vatten & Miljö i Väst AB, P.O. Box 110, SE-311 22 Falkenberg, Sweden

[e]Water Resources Engineering, Department of Building and Environmental Technology, Lund University, P.O. Box 118, SE-221 00 Lund, Sweden

[*]Corresponding author: catherine.paul@tvrl.lth.se

[1]Present address: Sydvatten AB, Hyllie Stationstorg 21, SE-215 32 Malmö, Sweden

Table of contents

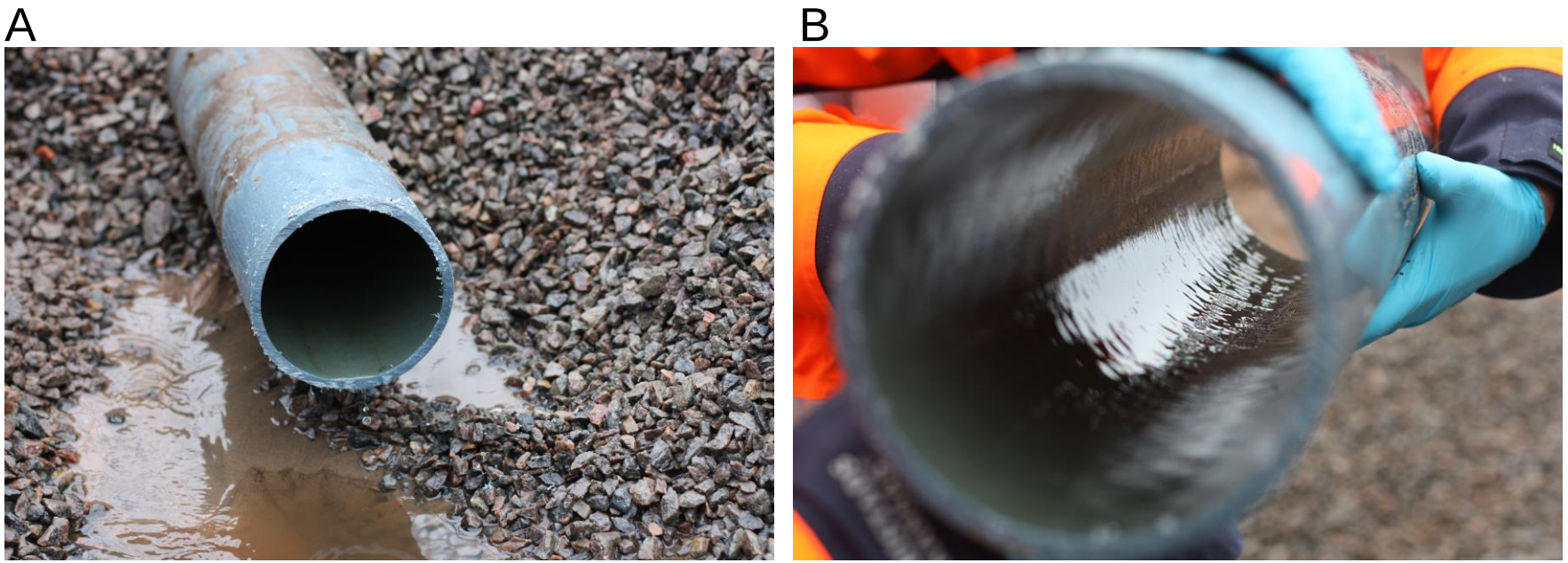

Figure S.1. (A) Cut DWDS pipe. (B) Pipe section brought to the lab.

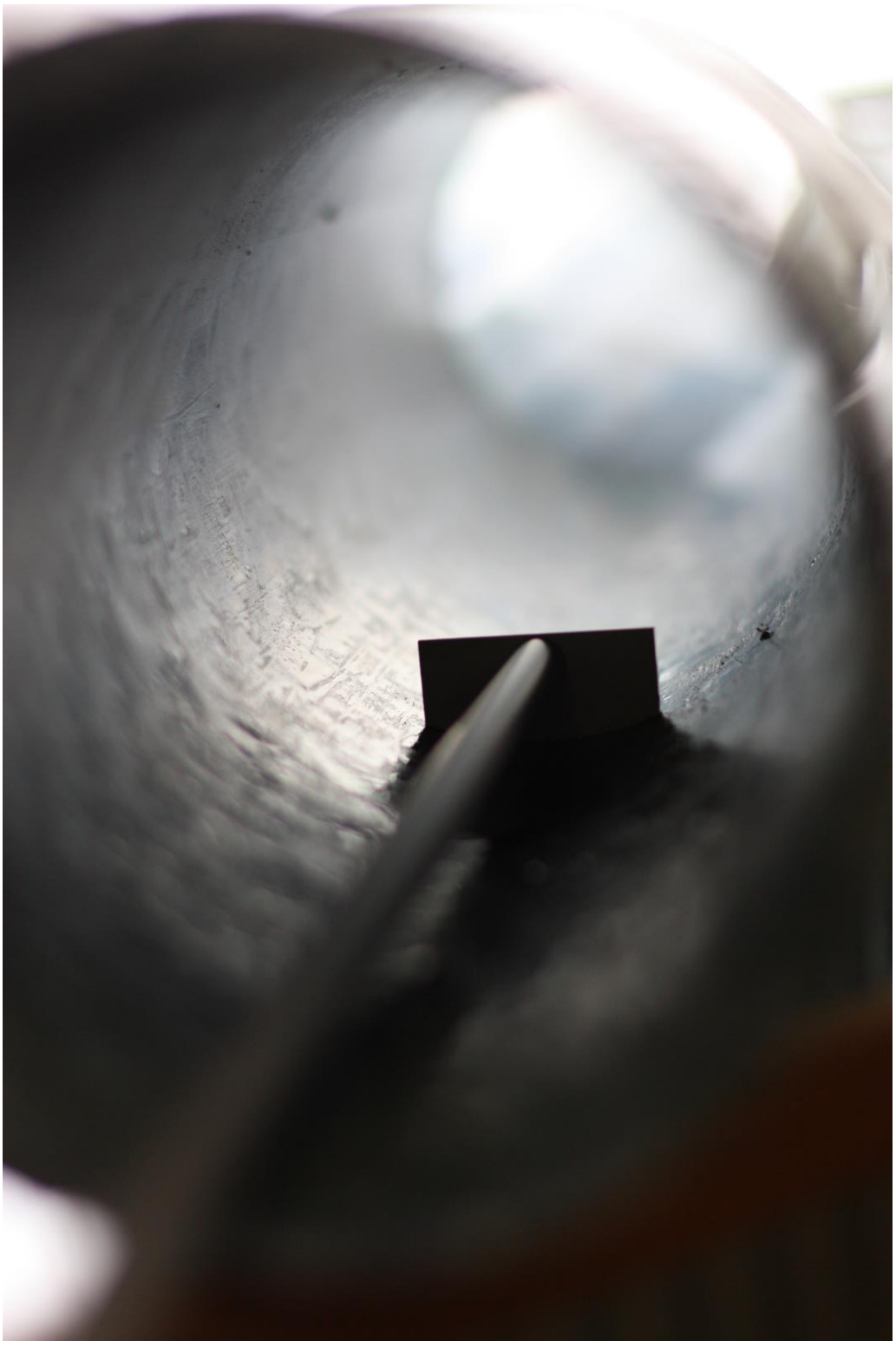

Figure S.2. Custom-made metal scrape used for biofilm collection.

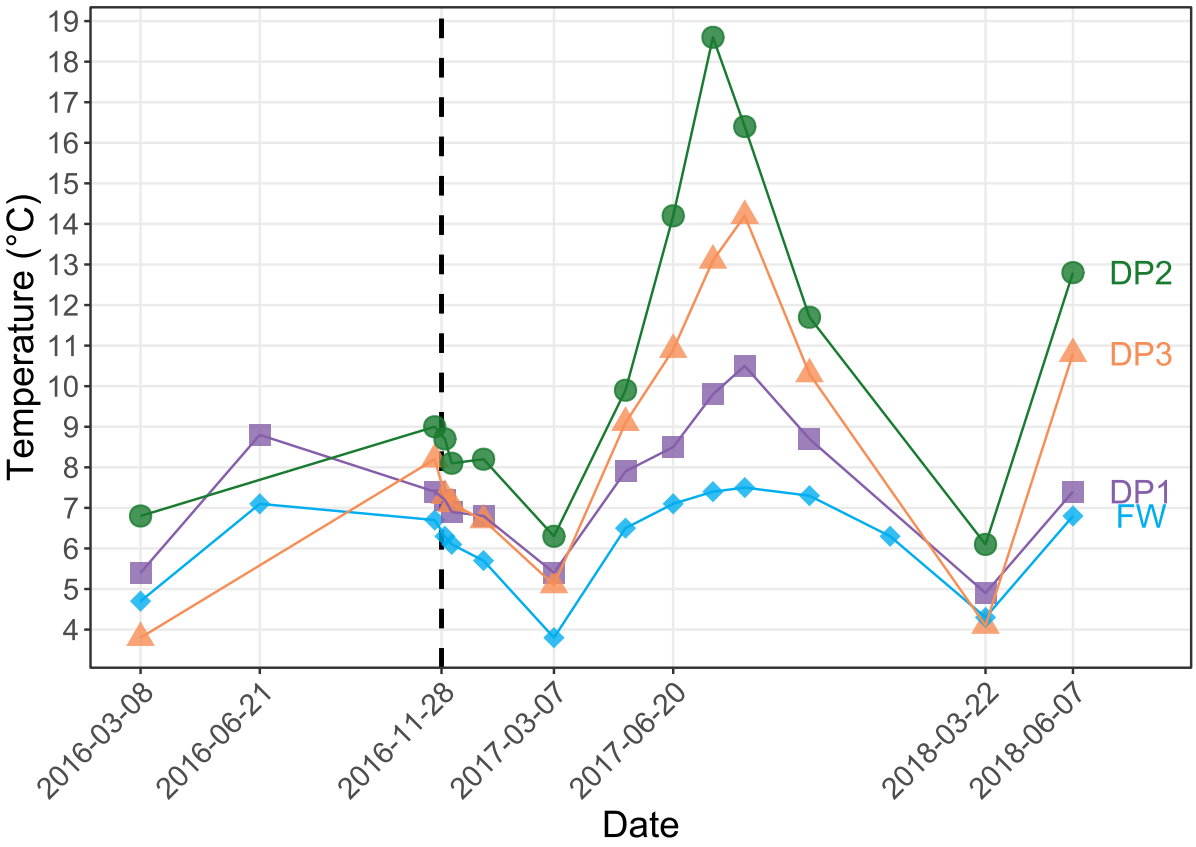

Figure S.3. Water temperatures of the water samples. Dashed vertical line represents the start of the UF, 2016-11-28.

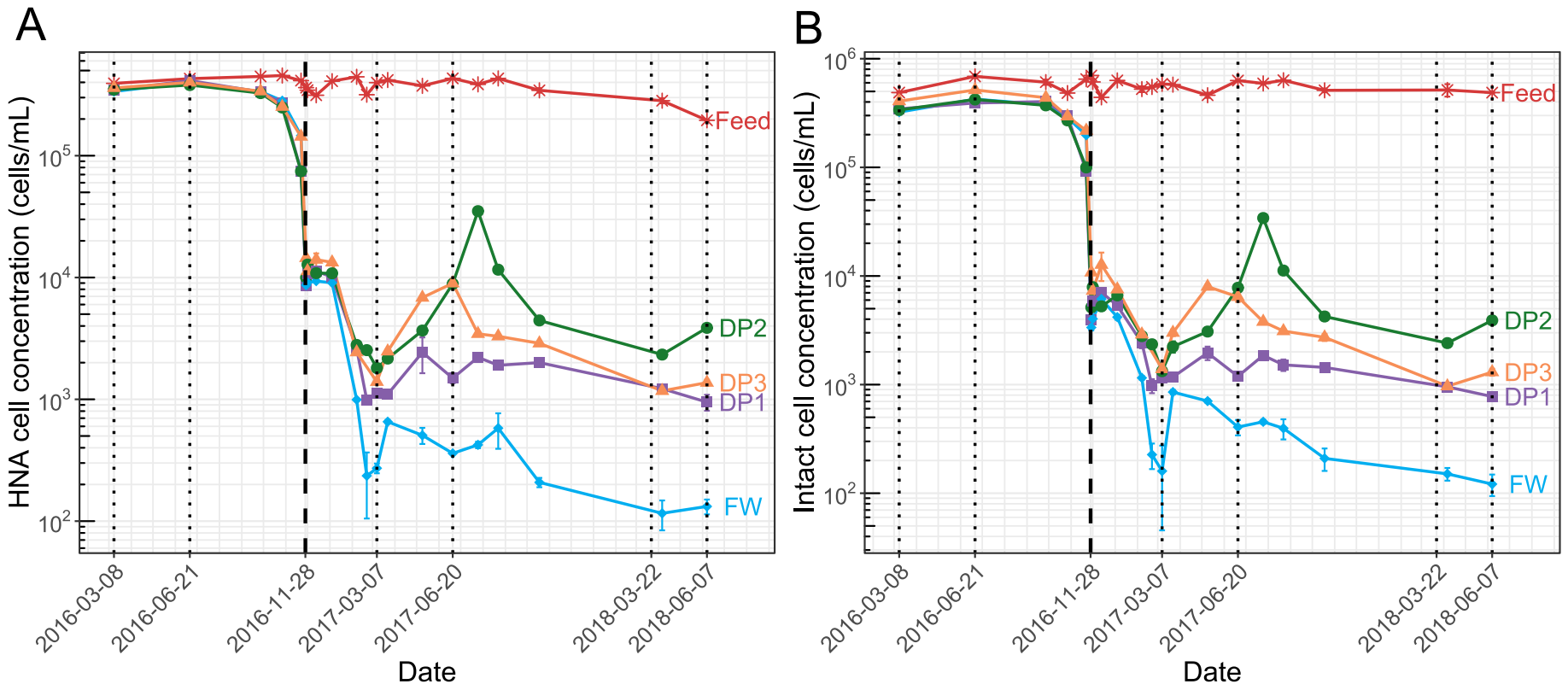

Figure S.4. (A) HNA cell concentration of the water samples. (B) Intact cell concentration of the water samples. (A,B) Error bars show standard deviations in technical triplicates. Dashed vertical line represents the start of the UF, 2016-11-28 and dotted vertical lines represent the biofilm sampling dates.

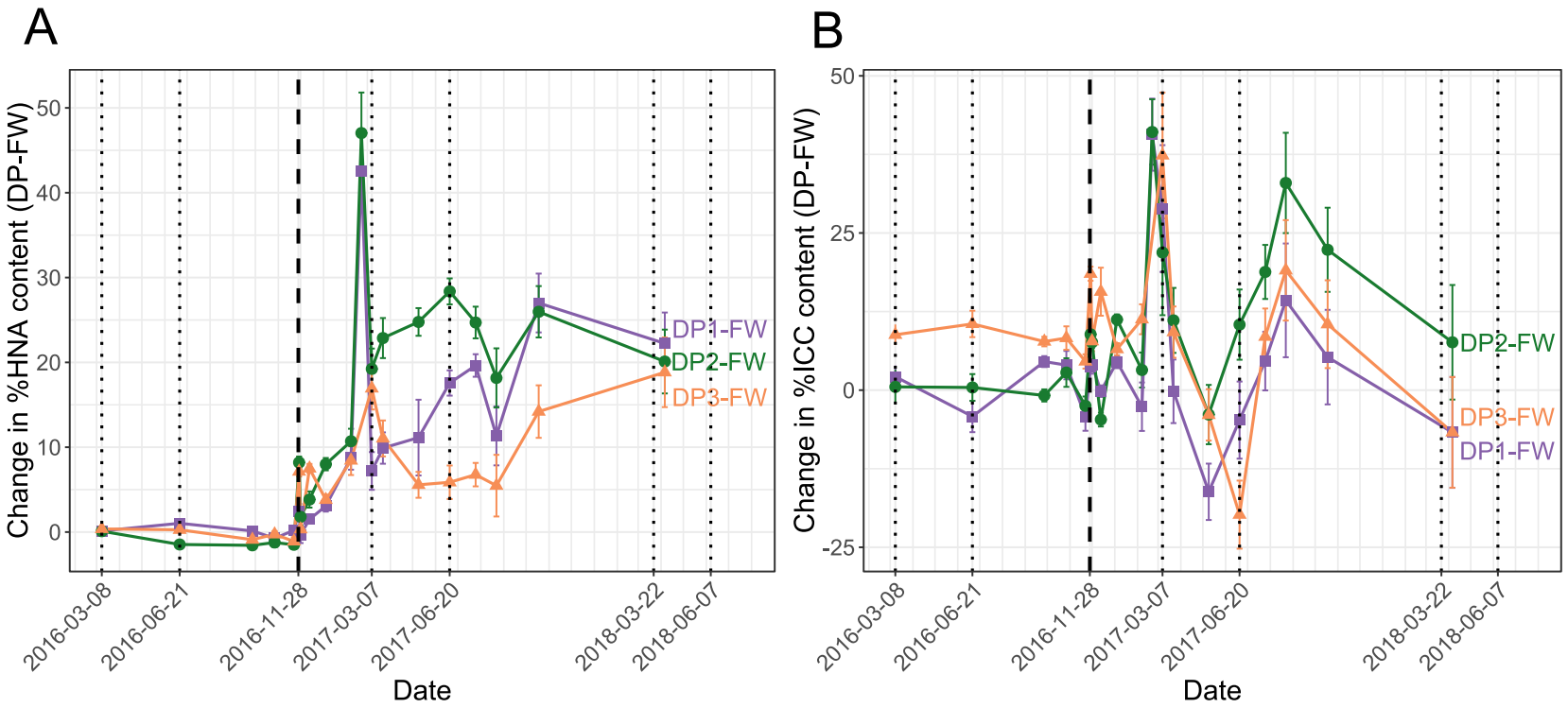

Figure S.5. (A) Change in the %HNA content, taking the %HNA DP and subtracting with the %HNA in FW. (B) Change in the %ICC content, taking the %HNA DP and subtracting with the %HNA in FW. (A,B) Error bars show standard deviations in technical triplicates. Dashed vertical line represents the start of the UF, 2016-11-28 and dotted vertical lines represent the biofilm sampling dates.

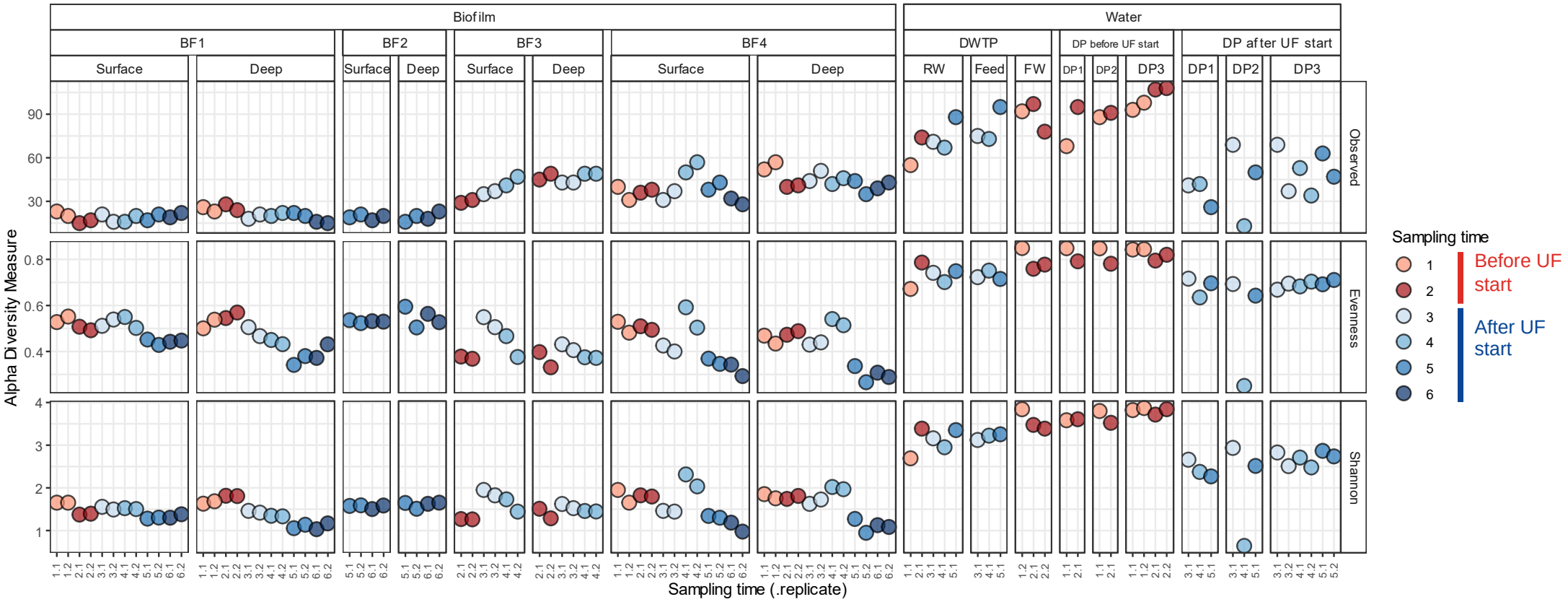

Figure S.6. The alpha diversity measures, observed ASVs, Evenness and Shannon index for the biofilm and water samples. Samples are ordered in rows and grouped together based on sample type. Sampling time indicates the date of sampling (Fig. 1B), samples indicated with red and blue are samples before UF and after UF start, respectively. Each point is one biological replicate.

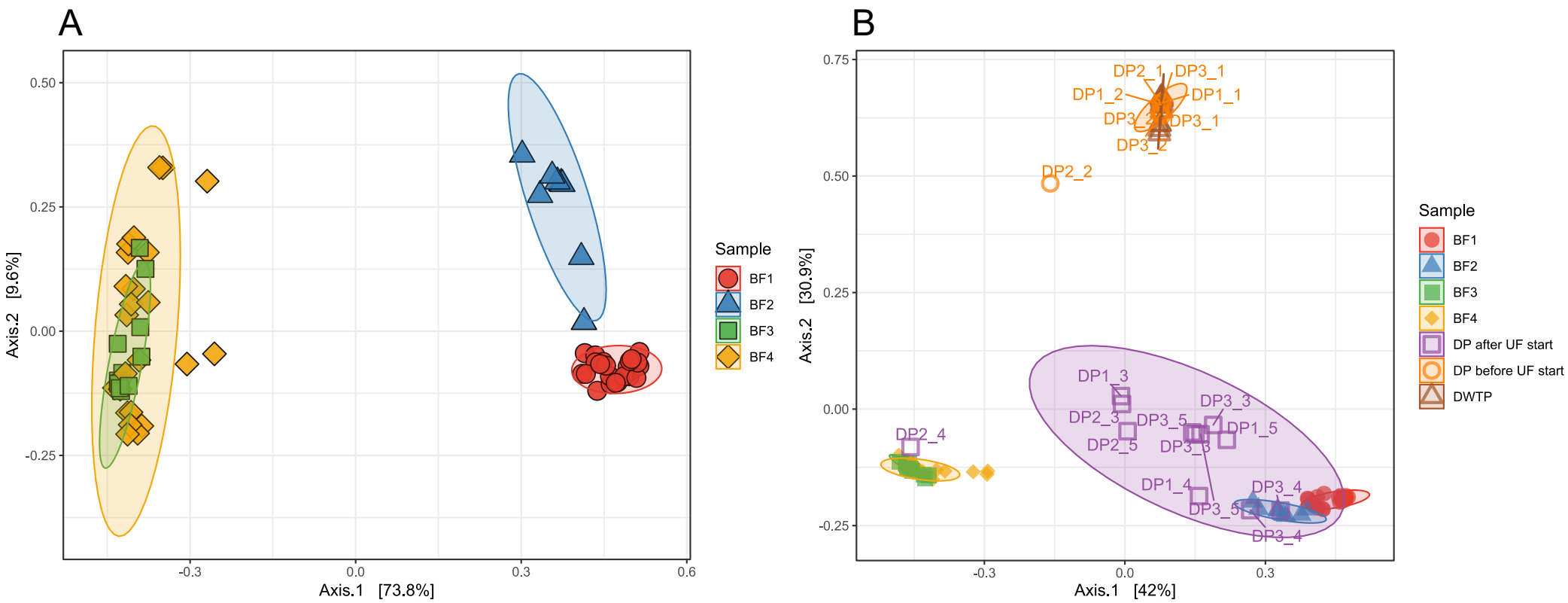

Figure S.7. Principal coordinates analysis (PCoA) plot based on Bray Curtis-dissimilarity of the bacterial communities. (A) Showing only biofilm samples. (B) Showing biofilm and water samples, DPs are indicated with the DP number following underscore and sampling time. (A,B) The transparent areas show the 95% confidence interval of the sample groups. BF1: n = 24, BF2: n = 8, BF3: n = 12, BF4: n = 24, DP after UF start: n = 12, DP before UF start: n = 8 and DWTP: n = 11. Due to uneven dispersion among groups (betadisper > 0.05 in Vegan package), clusters formed could not be confirmed by permutational analyses.

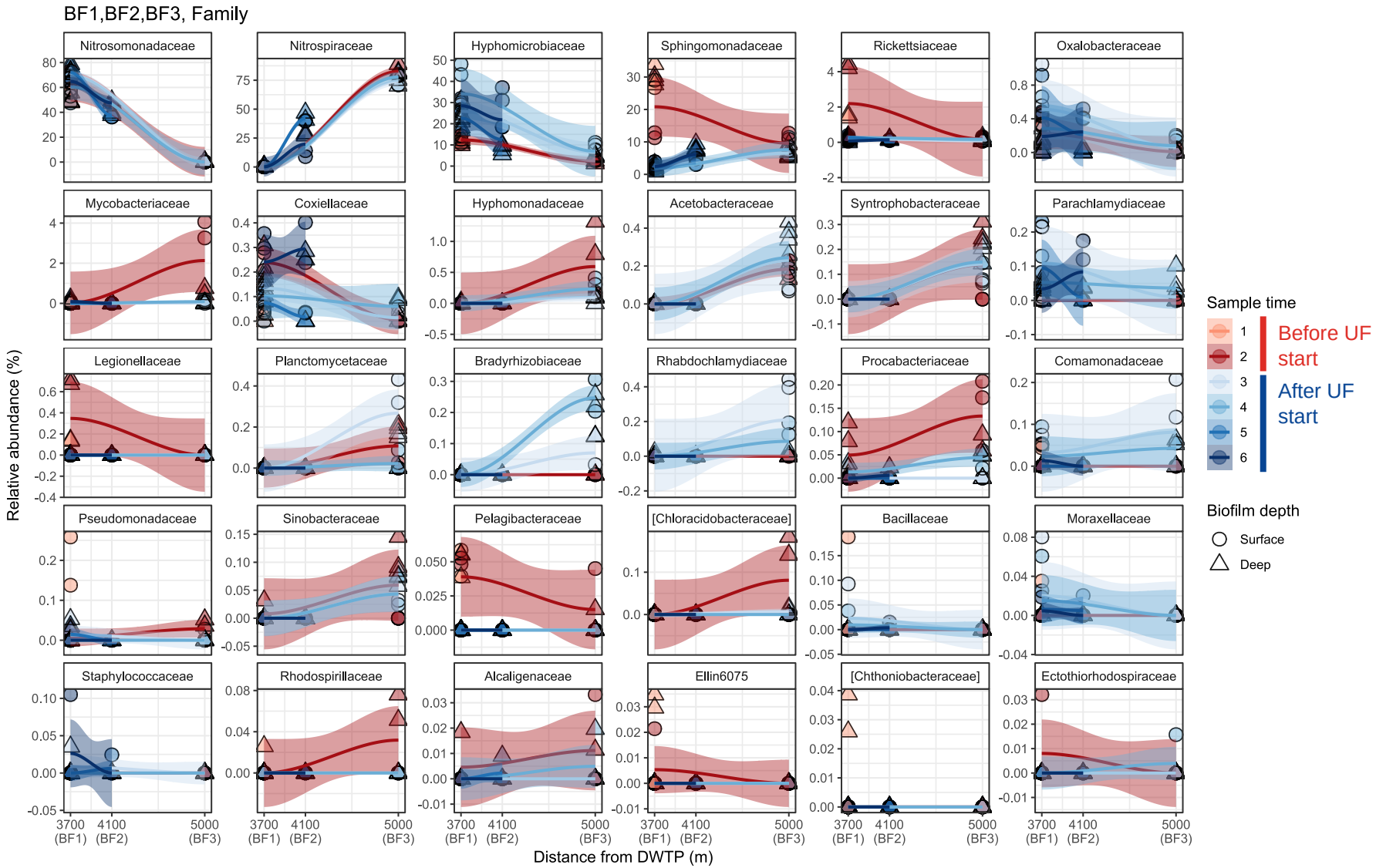

Figure S.8. Impact of distance (BF1, BF2 and BF3) from the DWTP on pipe biofilm taxa at family level. The taxa are ordered with greatest relative abundance in top left panel with subsequent decrease. Sample time 1 and 2 (red) indicate before UF start and 3,4,5 and 6 (blue) indicate after UF start. Blue and red lines show locally weighted least squares (loess) regression for each sample time and the transparent areas show the 95% confidence interval for each loess regression. n = 2 for both surface and deep biofilm at every sampling time.

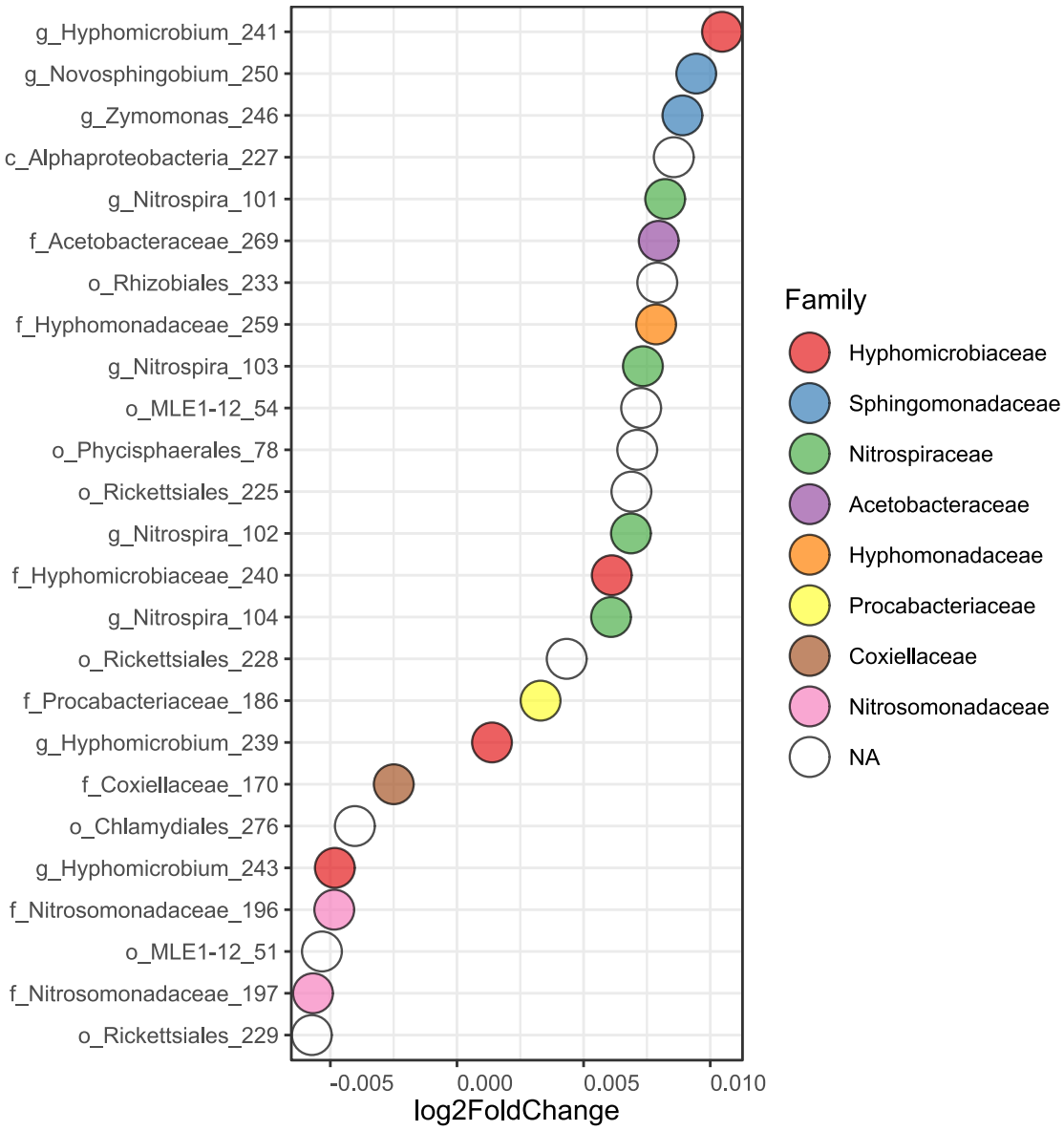

Figure S.9. Differential abundance analysis using DESeq2 ($P_{adjusted} < 0.05$), where BF1 (n = 24, BF2 (n = 8) and BF3 (n = 12) were used and the distance from the DWTP in meters were used as parameter. Positive log2fold change indicate ASV increase with distance.

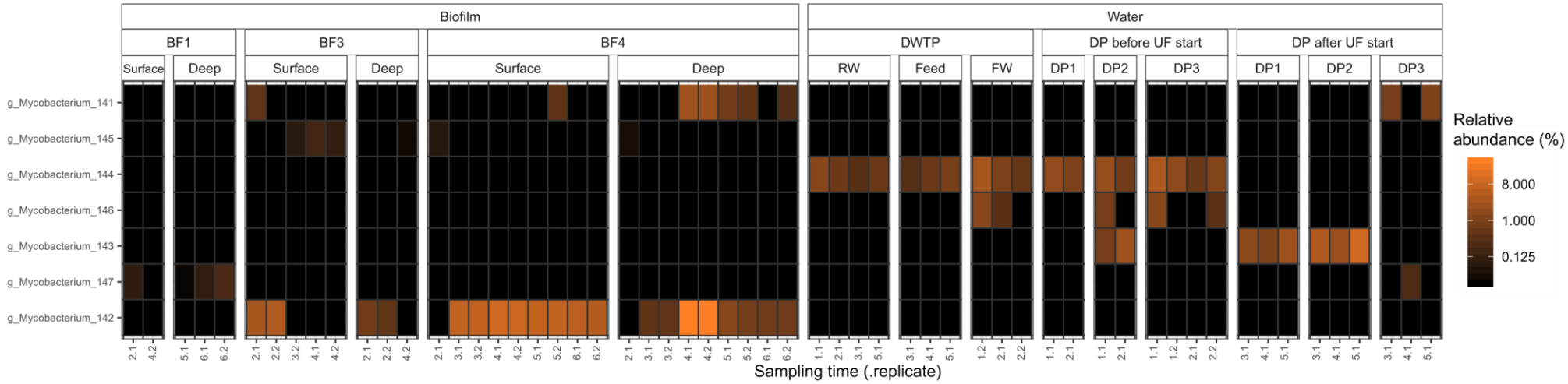

Figure S.10. Heatmap showing only samples with ASVs classified within family *Mycobacteriaceae*. Samples are ordered in rows and grouped together based on sample type. Each column is one biological replicate.

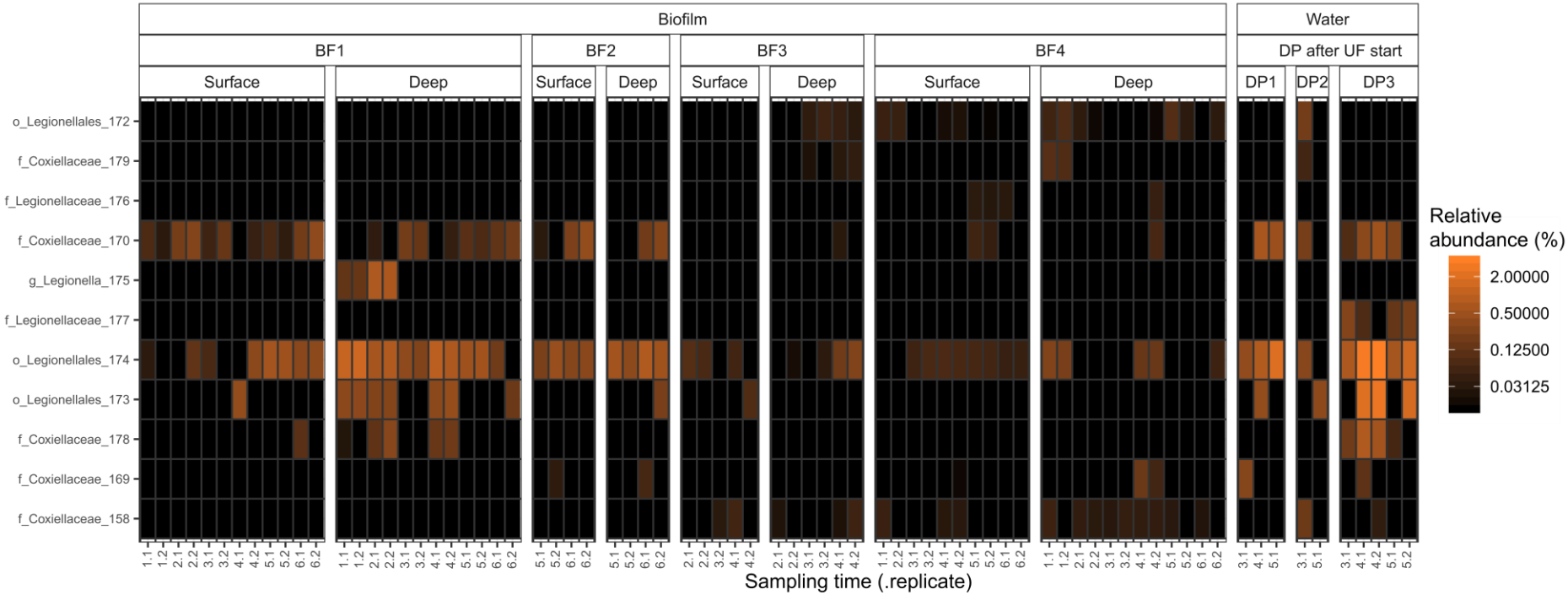

Figure S.11. Heatmap showing only samples with ASVs classified within order *Legionellales*. Samples are ordered in rows and grouped together based on sample type. Each column is one biological replicate.

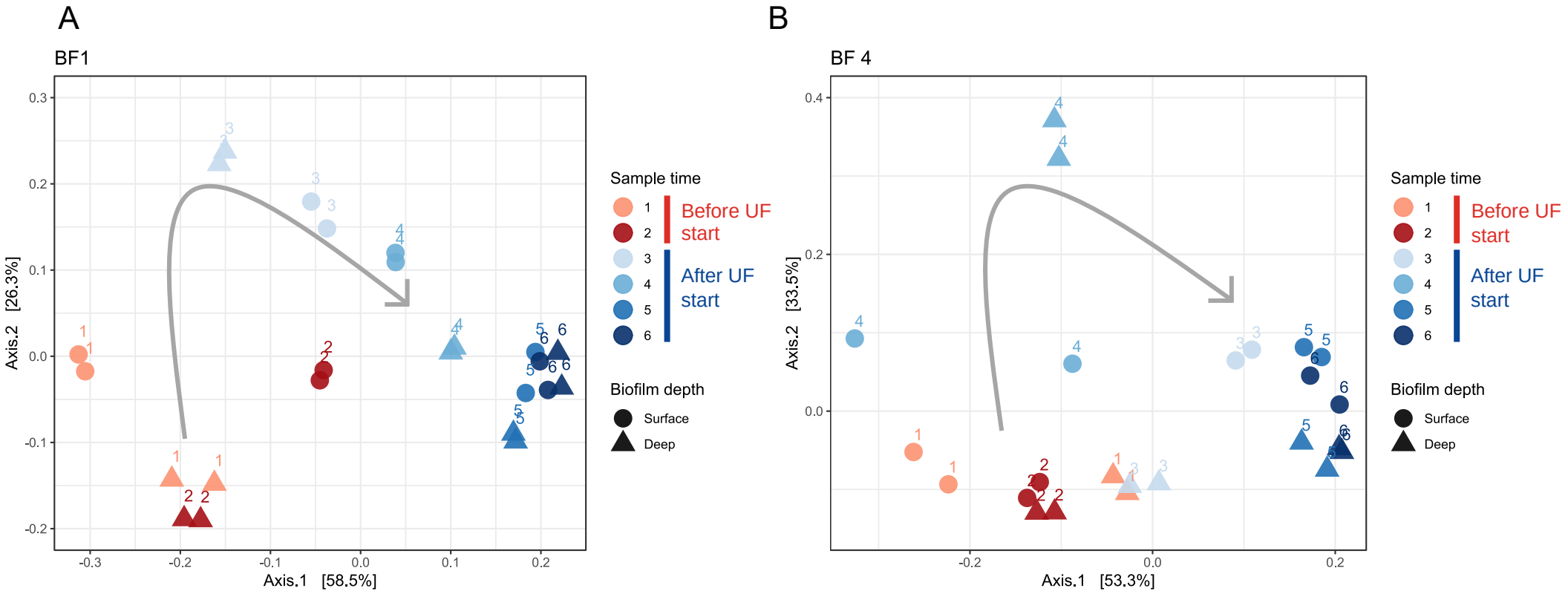

Figure S.12. Principal coordinates analysis (PCoA) plot based on Bray Curtis-dissimilarity of the bacterial communities. (A) Showing only BF1. (B) Showing only BF4. (A,B) The grey arrows indicate the progression of samples over time. Samples indicated with red and blue are samples before UF and after UF start, respectively. n = 2 for both surface and deep biofilm at every sampling time.

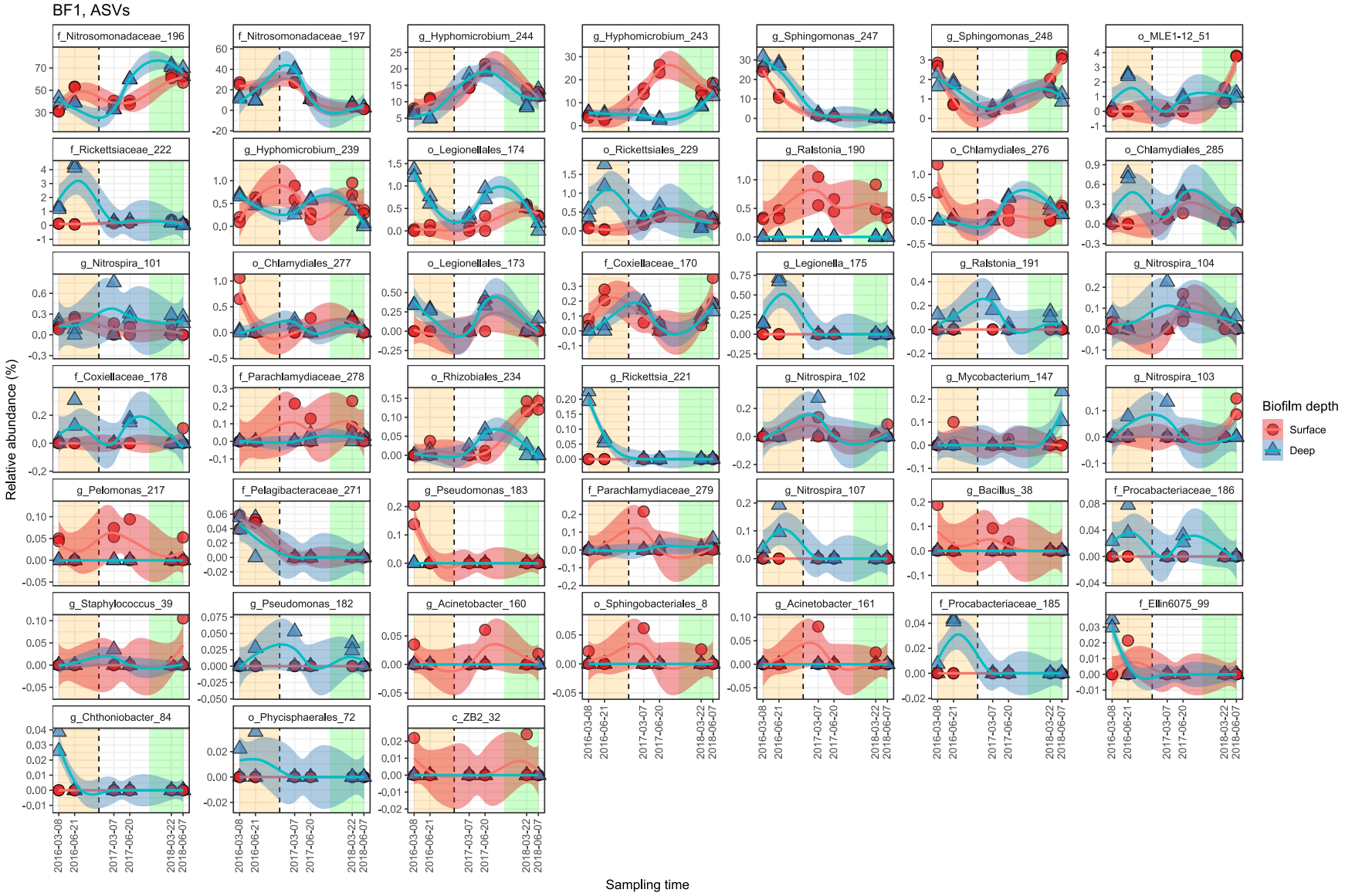

Figure S.13. Dynamics of all ASVs in BF1 over time. The ASVs are ordered with greatest relative abundance in top left panel with subsequent decrease. Vertical dashed line indicates the UF start. Orange, white and green background indicate before UF, transition state and after UF periods, respectively. ASVs are shown with the most specified taxonomy when available, g = genus, f = family, o = order and c = class. Dates indicate the six sampling times. Blue and red lines show locally weighted least squares (loess) regression for each biofilm depth and the transparent areas show the 95% confidence interval for each loess regression. n = 2 for both surface and deep biofilm at every sampling time.

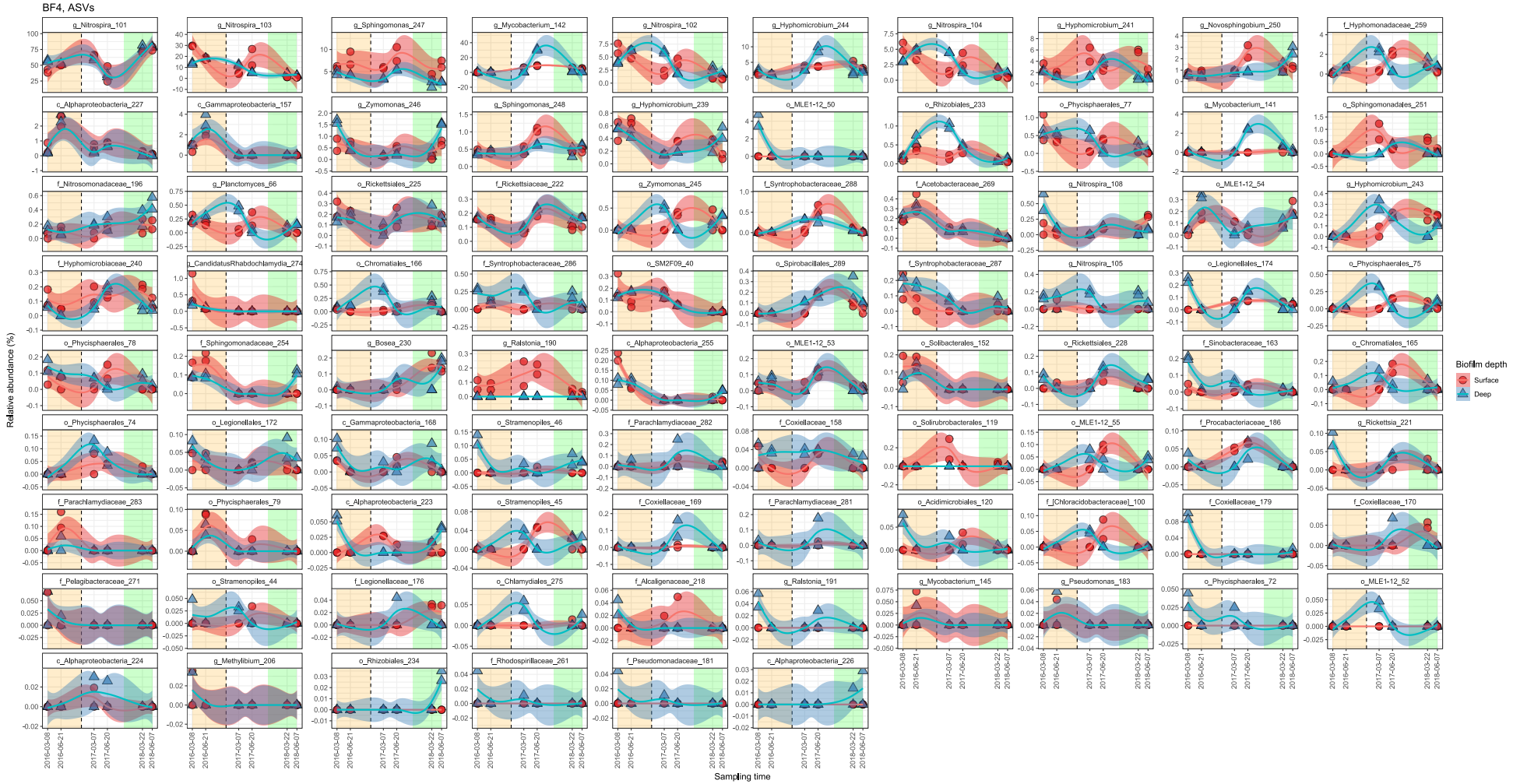

Figure S.14. Dynamics of all ASVs in BF4 over time. The ASVs are ordered with greatest relative abundance in top left panel with subsequent decrease. Vertical dashed line indicates the UF start. Orange, white and green background indicate before UF, transition state and after UF periods, respectively. ASVs are shown with the most specified taxonomy when available, g = genus, f = family, o = order and c = class. Dates indicate the six sampling times. Blue and red lines show locally weighted least squares (loess) regression for each biofilm depth and the transparent areas show the 95% confidence interval for each loess regression. n = 2 for both surface and deep biofilm at every sampling time.

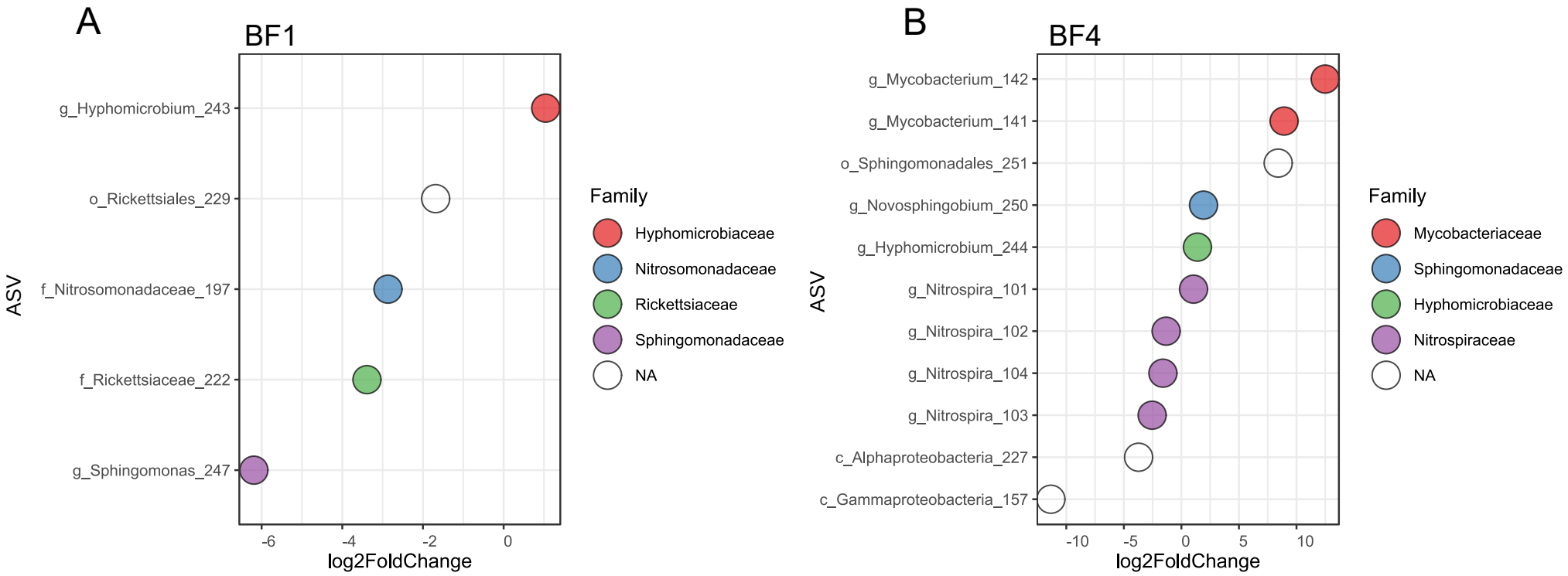

Figure S.15. Differential abundance analysis using DESeq2 ($P_{adjusted} < 0.05$), comparing sampling time 1 and 2 (before UF) to sampling time 5 and 6 (after UF) using only ASVs > 1.2% in one sample, as in figure 5. (A) Log_2fold changes of ASVs in BF1. (B) Log_2fold changes of ASVs in BF4.

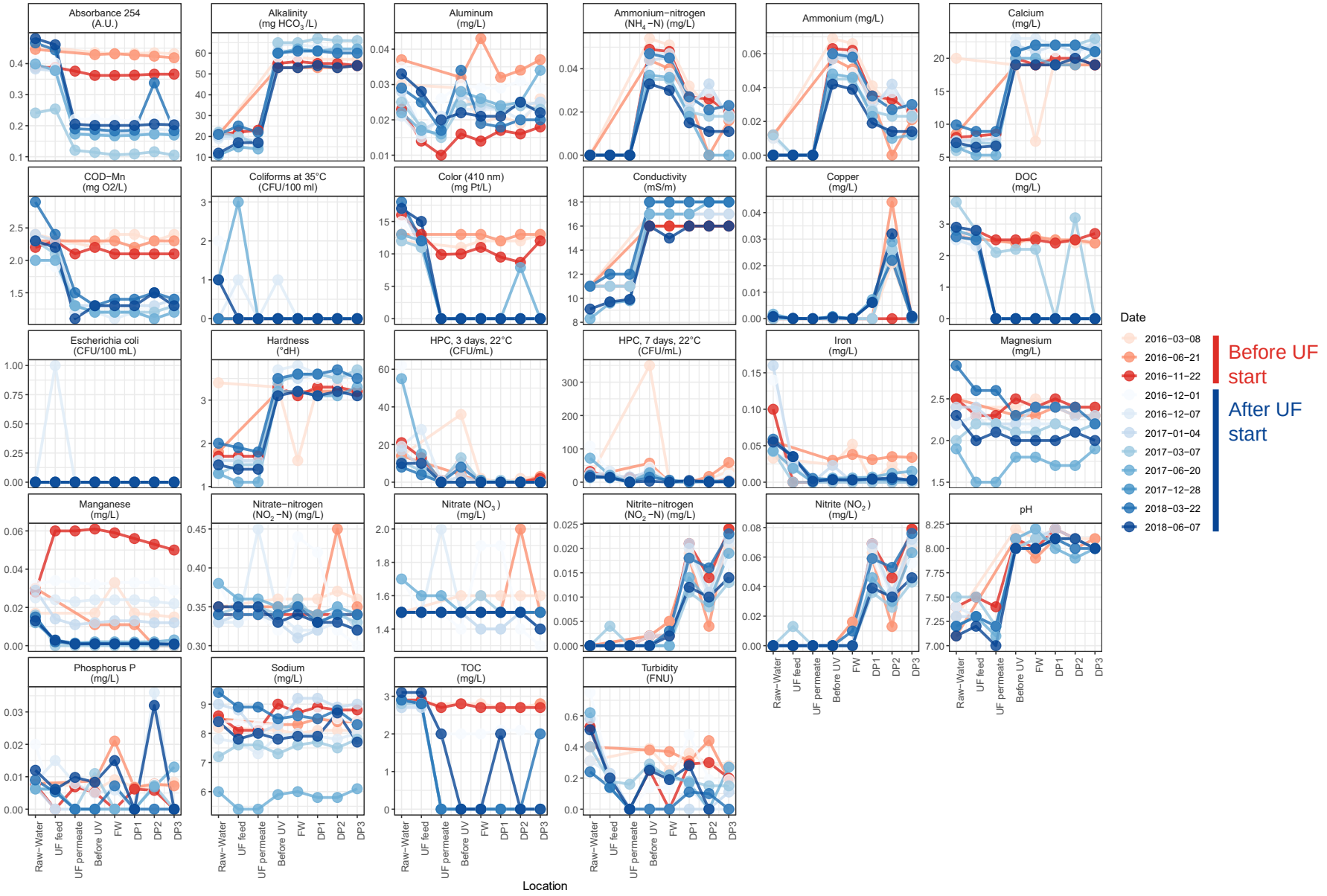

Figure S.16. Conventional chemical analyses on the water samples. Dates indicated with red and blue are samples before UF and after UF start, respectively. Limit of quantification for various analyses was; ammonium-nitrogen: 0.01 mg/L, ammonium: 0.01 mg/L, color: 5.0 mg Pt/L, copper: 0.02 mg/L, DOC: 2.0 mg/L, iron: 0.02 mg/L, manganese: 0.01 mg/L, nitrite-nitrogen: 0.002 mg/L, nitrite: 0.007 mg/L, phosphorus: 0.005 mg/L, TOC: 2.0 mg/L and turbidity: 0.1 FNU, depicted as 0 in the figure. n = 1 for every sampling time.

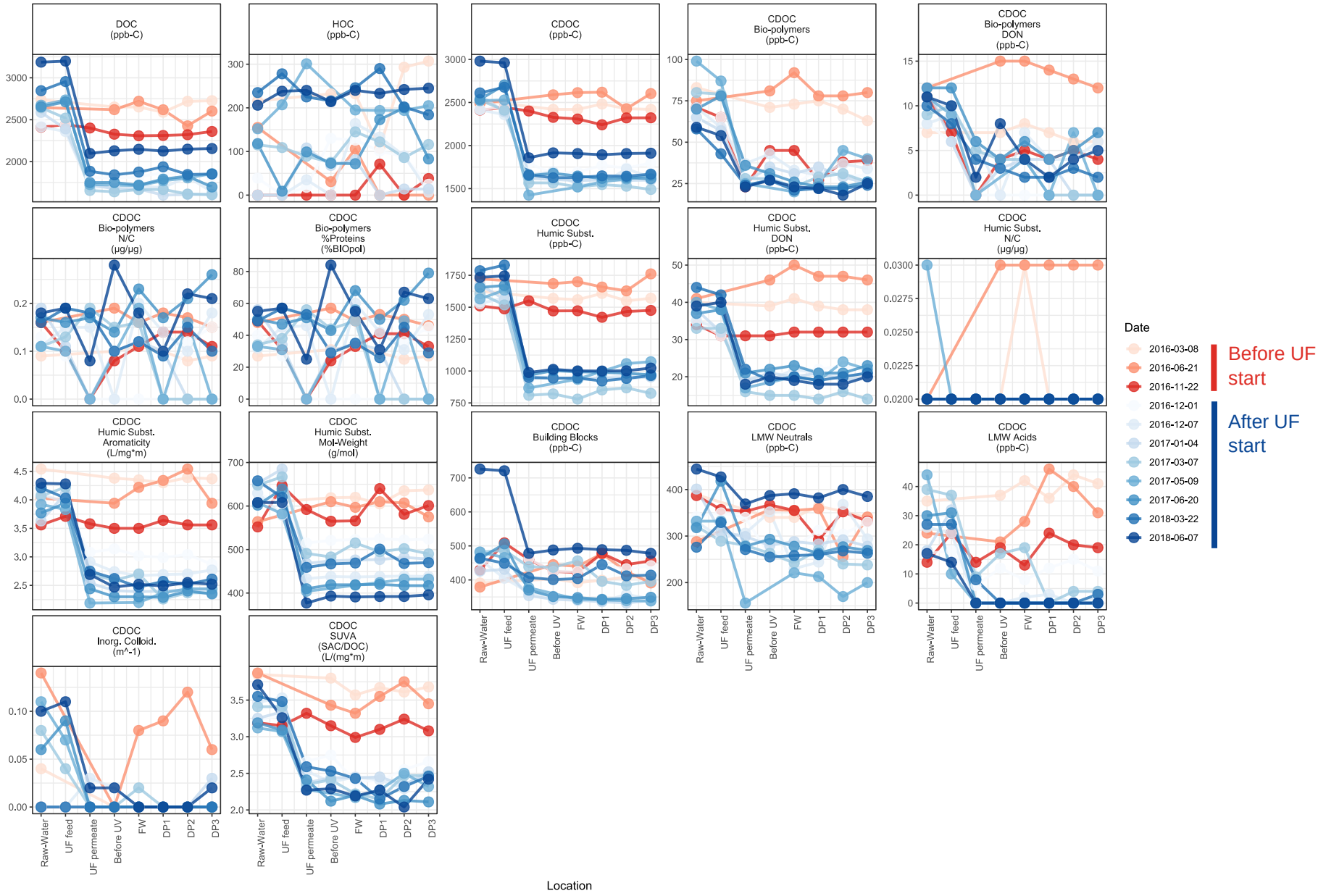

Figure S.17. NOM analyses by LC-OCD-OND on the water samples. Dates indicated with red and blue are samples before UF and after UF start, respectively. Abbreviations; DOC: dissolved organic carbon, HOC: hydrophobic organic carbon, CDOC: chromatographic dissolved organic carbon, DON: dissolved organic nitrogen and SAC: spectral absorption coefficient. 1000 ppb = 1 mg/L. n = 1 for every sampling time.

Table S.1. Shared core communities between the biofilm samples from Fig. 4. Abbreviations; ∩ = intersection, ∪ = union and \ = set subtraction.

BF1∩BF2∩BF3∩BF4	(BF2∩BF3∩BF4)\(BF1)	(BF1∩BF3∩BF4)\(BF2)	(BF3∩BF4)\(BF1∪BF2)	(BF1∩BF2∩BF4)\(BF3)	(BF4)\(BF1∪BF2∪BF3)	(BF3)\(BF1∪BF2∪BF4)	(BF1∩BF2)\(BF3∪BF4)	(BF1)\(BF2∪BF3∪BF4)
f_Nitrosomonadaceae_196	o_MLE1-12_54	g_Nitrospira_101	g_Planctomyces_66	o_Legionellales_174	o_SM2F09_40	o_Stramenopiles_46	o_MLE1-12_51	o_Legionellales_173
f_Rickettsiaceae_222	g_Nitrospira_102		o_Phycisphaerales_78	g_Ralstonia_190	o_Phycisphaerales_75	o_MLE1-12_50	f_Coxiellaceae_170	g_Legionella_175
g_Hyphomicrobium_239	g_Nitrospira_103		g_Nitrospira_104	g_Hyphomicrobium_243	o_Phycisphaerales_77	g_Nitrospira_106	f_Nitrosomonadaceae_197	f_Coxiellaceae_178
g_Hyphomicrobium_244			g_Nitrospira_105		g_Mycobacterium_141			g_Ralstonia_191
g_Sphingomonas_247			g_Nitrospira_108		o_Solibacterales_152			o_Rickettsiales_229
g_Sphingomonas_248			g_Mycobacterium_142		o_Chromatiales_166			o_Rhizobiales_234
			c_Gammaproteobacteria_157		f_Hyphomicrobiaceae_240			o_Chlamydiales_276
			o_Rickettsiales_225		g_Zymomonas_245			o_Chlamydiales_277
			c_Alphaproteobacteria_227		o_Sphingomonadales_251			o_Chlamydiales_285
			g_Bosea_230		f_Syntrophobacteraceae_287			
			o_Rhizobiales_233		f_Syntrophobacteraceae_288			
			g_Hyphomicrobium_241		o_Spirobacillales_289			
			g_Zymomonas_246					
			g_Novosphingobium_250					
			f_Sphingomonadaceae_254					
			c_Alphaproteobacteria_255					
			f_Hyphomonadaceae_259					
			f_Acetobacteraceae_269					
			g_CandidatusRhabdochlamydia_274					
			f_Syntrophobacteraceae_286					